Available online at www.sciencedirect.com
SCIENCE DIRECT®
Journal of Organometallic Chemistry 690 (2005) 3774–3782
Journal of Organometallic Chemistry
www.elsevier.com/locate/jorganchem

Intramolecular hydroamination of 6-aminohex-1-yne catalyzed by Lewis acidic rhenium(I) carbonyl complexes

Ling Ling Ouh [a], Thomas Ernst Müller [b,1], Yaw Kai Yan [a,*]

[a] *Natural Sciences and Science Education, National Institute of Education, Nanyang Technological University, NIE Blk 7 Science, 1 Nanyang Walk, Singapore 637616, Singapore*

[b] *Department of Chemistry, National University of Singapore, Faculty of Science, 3 Science Drive 3, Singapore 117543, Singapore*

Received 28 March 2005; received in revised form 9 May 2005; accepted 9 May 2005
Available online 16 June 2005

Abstract

With the aim to determine the effect of Lewis acidity of rhenium(I) carbonyl complexes on their catalytic properties, and to develop more efficient catalysts based on Re(I) carbonyl systems, a series of rhenium(I) carbonyl triflate complexes with various degrees of Lewis acidity was investigated. Pyridine-substituted bromo tricarbonyl rhenium(I) complexes of the type *fac*-$[ReBr(CO)_3L_2]$ (L = py-Cl, py, py-Me and py-NMe_2) were synthesized from $[ReBr(CO)_5]$ using trimethylamine *N*-oxide (TMNO) as decarbonylating agent. The complexes $[ReBr(CO)_5]$ and *fac*-$[ReBr(CO)_3L_2]$ were then reacted with silver triflate to yield the complexes $[Re(CF_3SO_3)(CO)_5]$ and *fac*-$[Re(CF_3SO_3)(CO)_3L_2]$. The synthesis and characterization of these complexes and their application in the catalysis of the cyclization of 6-aminohex-1-yne are discussed. The crystal structure of $[Re(CF_3SO_3)(CO)_3(py)_2]$ is also presented.

Keywords: Hydroamination; Catalysis; Rhenium carbonyl complex; Lewis acid; Triflate; Pyridine

1. Introduction

As valuable and important industrial chemicals, amines, enamines and imines are produced *via* several different routes [1]. Among them the direct formation of a new C–N bond by addition of an amine to an unsaturated C–C bond, i.e., hydroamination, could be of great significance [2–5]. The hydroamination reaction offers an atom-efficient pathway to primary, secondary, and tertiary amines, as well as enamines and imines, directly from alkenes and alkynes. While the reaction is thermodynamically feasible [6–8], there is a high energy barrier under normal conditions, necessitating the use of a catalyst.

Various metals, especially early (e.g., Ti [9,10], lanthanides [11]) and late transition metals [12] (e.g., Ni [13], Rh [14], Pd [15]) are known to catalyze hydroamination reactions. In earlier investigations on catalytic hydroamination, complexes of group 5–8 metals were conspicuous by their absence [16,17]. In particular, there is only one report on the use of rhenium complexes for catalysis of hydroamination reactions, wherein the complex $[Re(CO)_5(H_2O)]BF_4$ was tested for its catalytic properties towards the cyclization of 6-aminohex-1-yne (**1**) [16]. Cyclization of **1** first generates the intermediate enamine 2-methylenepiperidine (**2**). Subsequent 1,3-hydrogen shift converts **2** into the more stable imine 2-methyl-1,2-dehydropiperidine (**3**) [18]. The use of $[Re(CO)_5(H_2O)]BF_4$ as catalyst demonstrates that Lewis acidic rhenium(I) centers can catalyze intramolecular

* Corresponding author. Tel.: +65 6 790 3821; fax: +65 6 896 9414.
E-mail addresses: Thomas.Mueller@tum.de (T.E. Müller), ykyan@nie.edu.sg (Y.K. Yan).
[1] Permanent address: Technische Universität München, Department Chemie, Lichtenbergstraße 4, 85747 Garching, Germany.

0022-328X/$ - see front matter © 2005 Elsevier B.V. All rights reserved.
doi:10.1016/j.jorganchem.2005.05.011

addition of amines to alkynes. The presence of Lewis acidic sites seems to be a sufficient condition for catalytic activity toward hydroamination [19,20]; a plausible mechanism being activation of the C–C triple bond by π-coordination to the metal centre, followed by intramolecular nucleophilic attack of the amino group on C-2 [12,21], although a mechanism involving oxidative addition of the amino group followed by insertion of the alkynyl group into the M–N bond is also possible [19,22,23]. Amine activation by proton abstraction [11,24] seems unlikely since $[Re(CO)_5(H_2O)]BF_4$ is not basic, and no strongly basic ligands or reactants were present in the reaction mixture. Mechanisms that involve protonation of metal complexes to form metal hydride intermediates [13,15] are also unlikely in the absence of strong acids.

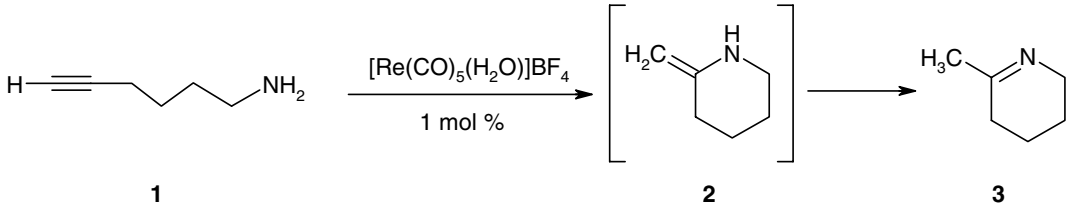

1 **2** **3**

Regardless of the mechanism, we expected that the Lewis acidity of rhenium(I) carbonyl complexes can be tuned with the incorporation of ligands of different electron-donating or withdrawing properties, and that this will influence the catalytic efficiency of the complexes. To examine this hypothesis, the complexes $[Re(CF_3SO_3)(CO)_5]$ and *fac*-$[Re(CF_3SO_3)(CO)_3L_2]$ [L = 4-chloropyridine (py-Cl), pyridine (py), 4-methylpyridine (py-Me), 4-(dimethylamino)pyridine (py-NMe_2)] were synthesized and tested for their catalytic properties towards the cyclization of **1** to **3**. The weakly bound triflate anion can readily dissociate to generate an empty coordination site, while the 4-substituted pyridines provide a homologous series of sterically equivalent ligands that differ only in their electron-donating/withdrawing properties. The results of this study, and the crystal structure of *fac*-$[Re(CF_3SO_3)(CO)_3(py)_2]$, are presented in this paper.

2. Experimental

2.1. Reagents and solvents

All reactions involving air- and/or moisture-sensitive compounds were routinely performed under nitrogen atmosphere using standard Schlenk techniques [25,26]. Solvents were of reagent grade and were vacuum degassed before use. Diethyl ether was distilled under nitrogen over sodium-benzophenone. Chemical reagents, unless otherwise stated, were used directly from commercial sources without any pretreatment. The compound 6-aminohex-1-yne was synthesized according to [27] and purified by distillation under reduced pressure before use. Preparative thin layer chromatography (TLC) was carried out on pre-coated silica plates of layer thickness 0.25 mm.

2.2. Instrumentation

Elemental analyses (C, H and N) were conducted using a LECO CHNS-932 instrument. Solution infrared absorption spectra were recorded in dichloromethane using a KBr cell of 0.1 mm path length with a Perkin–Elmer 1725X FT-IR spectrometer of operating region 4000–400 cm^{-1}. Solid-state spectra were recorded from KBr pellets. Proton NMR spectra were recorded at room temperature on a Bruker DRX400 spectrometer at 400 MHz, 5-mm tubes being used. Chemical shifts are quoted in ppm downfield of tetramethylsilane (TMS) as internal reference.

2.3. Syntheses

The complex $[ReBr(CO)_5]$ was prepared according to the method described in [28]. Yields, R_f values and elemental analysis data for the complexes $[ReBr(CO)_3L_2]$ and $[Re(CF_3SO_3)(CO)_3L_2]$ (L = CO, py-Cl, py, py-Me and py-NMe_2) are summarized in Table 1 while IR and ^1H NMR data are presented in Tables 2 and 3, respectively.

2.3.1. *fac*-[$ReBr(CO)_3(py\text{-}Cl)_2$]

Solid sodium bicarbonate (0.603 g, 7.18 mmol) was added to a solution of 4-chloropyridine hydrochloride (1.08 g, 7.18 mmol) in H_2O (5 cm^3). Once the effervescence had subsided, the 4-chloropyridine formed was extracted four times with Et_2O (2.5 cm^3). The collected extracts were combined and dried with anhydrous sodium sulphate. The mixture was then filtered and Et_2O was removed from the filtrate under reduced pressure.

The 4-chloropyridine obtained was dissolved in acetone (15 cm^3) and solid $TMNO \cdot 2H_2O$ (0.301 g, 2.71 mmol) added to the solution. Solid $[ReBr(CO)_5]$

Table 1
Yields and analytical data for $[ReBr(CO)_3L_2]$ and $[Re(CF_3SO_3)(CO)_3L_2]$

L	$[ReBr(CO)_3L_2]$					$[Re(CF_3SO_3)(CO)_3L_2]$			
	Yield (%)	R_f[b]	C(calc)[c] (%)	H(calc)[c] (%)	N(calc)[c] (%)	Yield (%)	C(calc)[c] (%)	H(calc)[c] (%)	N(calc)[c](%)
CO	80	0.82	14.9(14.8)	0.1(0)	0.0(0)	48	14.8(15.2)	0.2(0)	0.2(0)
py-Cl[a]	41	0.81	25.9(25.4)[d]	1.5(1.5)[d]	4.3(4.2)[d]	43	26.4(26.0)	1.4(1.3)	4.5(4.3)
py	60	0.59	30.9(30.7)	2.0(2.0)	5.6(5.5)	68	27.8(29.1)[f]	1.8(1.8)	5.2(4.9)
py-Me	81	0.72	33.3(33.6)	2.3(2.6)	5.4(5.2)	33	30.7(31.8)[f]	2.4(2.3)	4.9(4.6)
py-NMe_2	67	0.52	33.3(33.0)[e]	2.9(3.3)[e]	8.9(8.9)[e]	54	31.5(32.6)[f]	2.9(3.0)	8.6(8.5)

[a] Two other unidentified products were observed.
[b] TLC: CH_2Cl_2/hexane (90:10 v/v), silica.
[c] Observed value; calculated value in brackets.
[d] Calculated value based on the formula $[ReBr(CO)_3(py\text{-}Cl)_2] \cdot CH_2Cl_2$.
[e] Calculated value based on the formula $[ReBr(CO)_3(py\text{-}NMe_2)_2] \cdot CH_2Cl_2$.
[f] Carbon analyses consistently lower than calculated values, despite excellent agreement for the H and N analyses. Possibly due to the formation of a small amount of refractory rhenium carbide during combustion analysis.

Table 2
Solution (CH_2Cl_2) IR absorptions for $[ReBr(CO)_3L_2]$ and $[Re(CF_3SO_3)(CO)_3L_2]$ in the carbonyl stretching region (cm^{-1})

L	$[ReBr(CO)_3L_2]$	$[Re(CF_3SO_3)(CO)_3L_2]$
CO	2154(w), 2046(s), 1988(m)	2166(w), 2059(s), 2004(m)
py-Cl	2030(s), 1930(s), 1894(s)	2042(s), 1942(s), 1910(s)
py	2028(s), 1925(s), 1892(s)	2040(s), 1938(s), 1907(s)
py-Me	2026(s), 1922(s), 1889(s)	2038(s), 1935(s), 1905(s)
py-NMe_2	2019(s), 1910(s), 1880(s)	2030(s), 1922(s), 1895(s)

Table 3
^1H NMR data, δ (ppm), for $[ReBr(CO)_3L_2]$ and $[Re(CF_3SO_3)(CO)_3L_2]$, recorded in $CDCl_3$

L	$[ReBr(CO)_3L_2]$			$[Re(CF_3SO_3)(CO)_3L_2]$		
	H_α[a]	H_β[a]	Others	H_α[a]	H_β[a]	Others
py-Cl	8.74(m)	7.36(m)	–	8.45(m)	7.49(m)	–
py	8.83(m)	7.86(m)	7.35(m, H_γ[a])	8.54(m)	7.93(m)	7.45(m, H_γ[a])
py-Me	8.63(t)	7.13(d)	2.41(s, CH_3)	8.34(d)	7.22(d)	2.44 (s, CH_3)
py-NMe_2	8.30(m)	6.38(m)	3.03(s, NCH_3)	S1[b]: 8.13(m)	6.73(m)	3.26 (s, NCH_3)
				S2[b]: 8.02(m)	6.44(m)	3.06 (s, NCH_3)

[a] H_α, H_β, H_γ refer to the *ortho*, *meta* and *para* protons on the pyridine ring.
[b] Two sets of signals, S1 and S2, were observed in the ratio 1:4 for the solution of $[Re(CF_3SO_3)(CO)_3(py\text{-}NMe_2)_2]$ in $CDCl_3$.

(0.550 g, 1.35 mmol) was then added to the mixture. Immediate effervescence was observed. After 4 h of continuous stirring under N_2 at r.t., the solvent was removed under reduced pressure. The residue was redissolved in a minimal amount of CH_2Cl_2 and chromatographed on silica TLC plates using CH_2Cl_2/hexane (70:30 v/v). The product band was scraped off, extracted with acetone, and recrystallized from CH_2Cl_2/hexane to yield a white microcrystalline solid.

2.3.2. *fac*-[ReBr(CO)$_3$(py)$_2$]

Solid TMNO · $2H_2O$ (0.345 g, 3.10 mmol) was added to a solution of pyridine (0.626 cm^3, 7.83 mmol) in acetone (15 cm^3). Solid $[ReBr(CO)_5]$ (0.630 g, 1.55 mmol) was then added to the resultant mixture under N_2. After 4 h of continuous stirring under N_2 at r.t., the product was precipitated by addition of MeOH (30 cm^3) to the reaction mixture.

2.3.3. *fac*-[ReBr(CO)$_3$(py-Me)$_2$]

The procedure was similar to that of *fac*-$[ReBr(CO)_3(py)_2]$ except that 4-methylpyridine (0.630 g, 6.76 mmol) was used instead of pyridine, and that the product was isolated by TLC [CH_2Cl_2/hexane (90:10 v/v)] and recrystallized from CH_2Cl_2/hexane.

2.3.4. *fac*-[ReBr(CO)$_3$(py-NMe$_2$)$_2$]

The procedure was similar to that of *fac*-$[ReBr(CO)_3(py\text{-}Me)_2]$ except that 4-(dimethylamino)pyridine (0.842 g, 6.89 mmol) was used instead of 4-methylpyridine.

2.3.5. [Re(CF$_3$SO$_3$)(CO)$_5$]

A solution of $[ReBr(CO)_5]$ (0.302 g, 0.743 mmol) in dichloromethane (30 cm^3) was carefully degassed. Finely divided $Ag(CF_3SO_3)$ (0.382 g, 1.49 mmol) was added under N_2, and the mixture stirred at r.t. for 2 h in the

dark. The precipitate was removed by filtration and the solvent evaporated under reduced pressure. The residue was exposed to light for 2 h to decompose any remaining silver salts. The solid was extracted with CH_2Cl_2 (30 cm^3), fine particles removed by gravity filtration, the volume of the filtrate reduced to 5 cm^3 under reduced pressure, and 10 cm^3 of Et_2O added. White crystals of the product were formed upon cooling to −10 °C.

2.3.6. *fac*-[Re(CO)$_3$(CF$_3$SO$_3$)L$_2$] (L = py-Cl, py, py-Me and py-NMe$_2$)

Set-up and procedure were analogous to $[Re(CF_3SO_3)(CO)_5]$ except that in the synthesis of $[Re(CO)_3(CF_3SO_3)(py\text{-}Cl)_2]$, hexane was used to precipitate out the white crystals.

2.4. Crystal structure determination

The crystal data and refinement parameters for $[Re(CF_3SO_3)(CO)_3(py)_2]$ are summarized in Table 4. The crystals were grown from CH_2Cl_2/hexane by slow evaporation at 10 °C, and were mounted on glass fibers for data collection at 298(2) K. The data were collected in the $\theta/2\theta$ mode using a Siemens P4 diffractometer with Mo Kα radiation ($\lambda = 0.71073$ Å), and were corrected for absorption effects using ψ-scan data. The structure was solved by direct methods and refined by full-matrix least-squares on F^2. All non-hydrogen atoms were refined anisotropically. Hydrogen atoms were introduced in calculated positions with C–H = 0.96Å and assigned isotropic thermal parameters $U(H) = 1.2\,U_{eq}(C)$ and allowed to ride on their parent carbon atoms. All calculations were performed on a Pentium PC using the SHELXTL software package [29]. Selected bond lengths and angles are given in Table 5.

Table 4
Crystal data and refinement parameters for $[Re(CF_3SO_3)(CO)_3(py)_2]$

Empirical formula	$C_{14}H_{10}F_3N_2O_6ReS$
Formula weight	577.50
Crystal system	Orthorhombic
Space group	*Pccn*
Unit cell dimensions	
a (Å)	27.508(7)
b (Å)	8.288(2)
c (Å)	16.016(3)
V (Å^3)	3652(1)
Z	8
D_{calc} (Mg/m^3)	2.101
Absorption coefficient (mm^{-1})	6.833
F(000)	2192
Crystal size (mm)	0.15 × 0.3 × 0.3
θ Range for data collection (°)	1.48–27.50
Limiting indices	$-1 \leqslant h \leqslant 35$, $-1 \leqslant k \leqslant 10$, $-1 \leqslant l \leqslant 20$
Reflections collected	5302
Independent reflections (R_{int})	4201 (0.0369)
Maximum and minimum transmission	0.9863 and 0.7073
Data/restraints/parameters	3646/0/245
Goodness-of-fit on F^2	0.998
Final *R* indices [$I > 2\sigma(I)$]	$R_1 = 0.0432$, $wR_2 = 0.0656$
R indices (all data)	$R_1 = 0.1006$, $wR_2 = 0.0832$
Extinction coefficient	0.00057(4)
Largest difference in peak and hole (e Å^{-3})	0.560 and −0.555

Table 5
Selected bond lengths (Å) and bond angles (°) for $[Re(CF_3SO_3)(CO)_3(py)_2]$

Re(1)–C(12)	1.881(7)	S(1)–O(2)	1.415(6)
Re(1)–C(11)	1.904(9)	S(1)–O(3)	1.417(6)
Re(1)–C(13)	1.903(9)	S(1)–O(1)	1.463(5)
Re(1)–O(1)	2.194(4)	C(11)–O(11)	1.149(9)
Re(1)–N(1)	2.203(6)	C(12)–O(12)	1.146(8)
Re(1)–N(2)	2.208(6)	C(13)–O(13)	1.157(9)
C(12)–Re(1)–C(11)	86.4(3)	C(13)–Re(1)–N(1)	92.5(3)
C(12)–Re(1)–C(13)	86.6(3)	O(1)–Re(1)–N(1)	83.3(2)
C(11)–Re(1)–C(13)	90.1(4)	C(12)–Re(1)–N(2)	95.2(3)
C(12)–Re(1)–O(1)	178.1(2)	C(11)–Re(1)–N(2)	93.7(3)
C(11)–Re(1)–O(1)	94.8(3)	C(13)–Re(1)–N(2)	175.8(3)
C(13)–Re(1)–O(1)	94.8(3)	O(1)–Re(1)–N(2)	83.3(2)
C(12)–Re(1)–N(1)	95.4(3)	N(1)–Re(1)–N(2)	83.6(2)
C(11)–Re(1)–N(1)	176.9(3)	S(1)–O(1)–Re(1)	129.6(3)

2.5. Catalytic studies

The five rhenium carbonyl triflate complexes $[Re(CF_3SO_3)(CO)_5]$ and *fac*-$[Re(CF_3SO_3)(CO)_3L_2]$ (L = py, py-Me, py-NMe$_2$ and py-Cl) were each tested for their catalytic properties on the cyclization of **1**. In a typical procedure, a mixture of **1** (0.10 cm^3, 0.88 mmol), $[Re(CF_3SO_3)(CO)_3L_2]$ (8.8 μmol) and CH_3CN (25 cm^3) was heated at reflux for 20 h. After cooling to room temperature, the reaction mixture was treated with 5 cm^3 of 1 M HCl in Et_2O (5 mmol). The mixture was stirred for 10 min, after which the solvent was removed under reduced pressure in a warm water bath. The residue was redissolved in CD_3OD and analyzed by ^{1}H NMR spectroscopy using the following signals

Table 6
Conversion observed in the cyclization of **1** to **3** catalyzed by $[Re(CF_3SO_3)(CO)_5]$ and $[Re(CF_3SO_3)(CO)_3L_2]$

L	Conversion[a] (%)	
	CH_3CN[b]	Toluene[b]
CO	3	61
py-Cl	5	78
py	9	63
py-Me	18	56
py-NMe$_2$	7	46

[a] After 20 h of reflux.
[b] Refluxing temperatures for CH_3CN: 82 °C, for toluene: 111 °C.

for integration: at δ 3.0 (2H) and 2.3 (3H) for the starting material **1** and at δ 3.6 (2H), 2.8 (2H) and 2.4 (3H) for the product **3**. The experiments were repeated in refluxing toluene. Percentage conversions of **1** to **3** obtained using the five complexes as catalysts are given in Table 6.

3. Results and discussion

3.1. Synthesis and characterization of fac-[ReBr(CO)$_3$L$_2$] (L = py-Cl, py, py-Me, py-NMe$_2$)

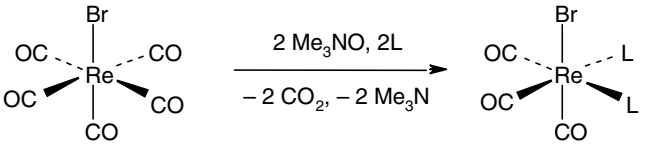

(L = py-Cl, py, py-Me, py-NMe$_2$)

The syntheses were carried out by adding [ReBr(CO)$_5$] to a mixture of TMNO and excess L in acetone. Interestingly, when [ReBr(CO)$_5$] was reacted with TMNO before adding L, poor yields of the target complexes were obtained. This could be because the intermediate complexes formed (probably [ReBr(CO)$_3$(NMe$_3$)$_2$] and/or [Re(μ-Br)$_2$(CO)$_8$]) are not very reactive with pyridines.

The spectroscopic data obtained for the complexes *fac*-[ReBr(CO)$_3$L$_2$] (L = py-Cl, py, py-Me, py-NMe$_2$) are consistent with the expected structures of the products. Three almost equally intense peaks are observed in the carbonyl stretching region of the IR spectra, consistent with a facial arrangement of the carbonyl groups (Table 2) [30]. The CO stretching frequencies for the complexes [ReBr(CO)$_3$(L)$_2$] decrease in the order L = CO > py-Cl > py > py-Me > py-NMe$_2$. It can therefore be deduced that the relative electron densities at the rhenium centre for the complexes [ReBr(CO)$_3$L$_2$] increase in the order L = CO < py-Cl < py < py-Me < py-NMe$_2$.

The chemical shifts of the pyridine protons H$_\alpha$ and H$_\beta$ decrease from L = py to L = py-NMe$_2$ (Table 3). This trend is as expected, since electron donating groups (Me, NMe$_2$) in *para* position intensify electron density in the vicinity of H$_\alpha$ and H$_\beta$. Unexpectedly, however, the α and β protons of [ReBr(CO)$_3$(py-Cl)$_2$] are more shielded than those of [ReBr(CO)$_3$(py)$_2$], despite the high electronegativity of Cl. It thus appears that there is significant electron-donation from Cl into the pyridine ring *via* the mesomeric effect. It must be noted, however, that *as a whole*, the 4-chloropyridine ligand donates *less* electron density to the Re centre than pyridine, as shown by the *higher* CO stretching frequencies of the 4-chloropyridine complex.

3.2. Synthesis and characterization of [Re(CF$_3$SO$_3$)(CO)$_5$] and fac-[Re(CF$_3$SO$_3$)(CO)$_3$L$_2$] (L = py-Cl, py, py-Me, py-NMe$_2$)

Silver triflate was used to remove the bromide ligand yielding the Lewis acidic rhenium carbonyl triflate salts [31]. The purification of the triflate complexes was, however, not as straightforward as that reported for [Re(CF$_3$SO$_3$)(CO)$_5$] (precipitation by addition of Et$_2$O followed by recrystallization from CH$_2$Cl$_2$/hexane). The product isolated by the reported procedure darkened rapidly on exposure to light, indicating contamination by silver salts. Therefore, the crude product was exposed to light for 2 h to decompose the silver salts to metallic silver. The residue was then re-extracted with CH$_2$Cl$_2$ and recrystallized from a mixture of CH$_2$Cl$_2$ and either Et$_2$O or hexane. The colorless crystals remain undarkened even after prolonged exposure to light.

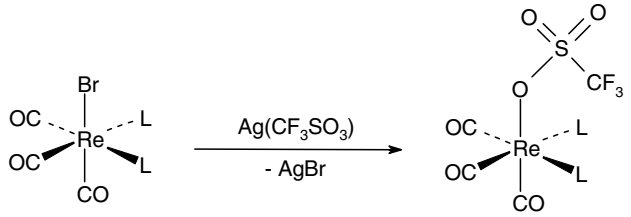

(L = CO, py-Cl, py, py-Me, py-NMe$_2$)

The IR spectra of the complexes [Re(CF$_3$SO$_3$)(CO)$_3$L$_2$] (L = py-Cl, py, py-Me, py-NMe$_2$) are similar to those of the bromo complexes in the carbonyl stretching region (Table 2). The CO stretching frequencies, and hence Lewis acidity, similarly decrease in the order L = CO > py-Cl > py > py-Me > py-NMe$_2$. Solid-state IR spectra obtained for the triflate complexes show C–F and S–O stretching peaks in the 1200–1300 cm^{-1} region [32], which are absent in the IR spectra of the corresponding bromo complexes. As expected, the CO stretching frequencies of the triflate complexes are higher than those of the bromo complexes, since the triflate anion is a poorer donor than bromide.

The relative electron-deficiency of the rhenium atoms of the triflate complexes also result in their β and γ protons being more deshielded than those of the corresponding bromide complexes (Table 3). Interestingly, however, the α protons of the triflate complexes are more shielded than those of the bromo complexes. This may be attributed to the shortening of the rhenium–pyridine bonds, due to increased electron donation from pyridine to rhenium, when the bromide ligand is replaced by triflate. The shortening of the rhenium–pyridine distance moves the α protons closer to/into the shielding region of the adjacent pyridine ring (Fig. 1), thus moving the α proton signal upfield. This

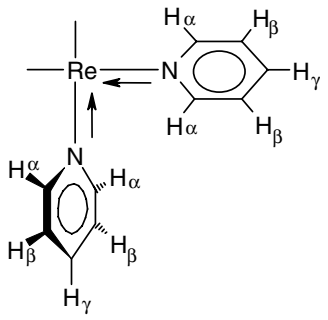

Fig. 1. Shortening of the rhenium–pyridine distances moves the α protons closer to/into the shielding region of the adjacent pyridine ring.

explanation is supported by the crystal structure of $[Re(CF_3SO_3)(CO)_3(py)_2]$ (see below).

It is also noteworthy that the ^1H NMR spectrum of $[Re(CF_3SO_3)(CO)_3(py\text{-}NMe_2)_2]$ shows two sets (S1 and S2 in Table 3) of py-NMe_2 proton signals in a 1:4 intensity ratio (the higher-field set, S2, is more intense). None of the other complexes reported herein exhibit this phenomenon. A plausible explanation for this phenomenon is that the complex $[Re(CF_3SO_3)(CO)_3(py\text{-}NMe_2)_2]$ is partially dissociated to the ion pair $[Re(CO)_3(py\text{-}NMe_2)_2]^+(CF_3SO_3)^-$, which gives rise to the lower-field set of ^1H signals, S1. This dissociation would be particularly facilitated by the py-NMe_2 ligand, since the NMe_2 group allows efficient delocalization of the positive charge on rhenium to both pyridine amine groups while maintaining an 18-electron configuration for the rhenium atom (Fig. 2). The very significant downfield shift of the NMe_2 proton signals of S1 relative to S2 and $[ReBr(CO)_3(py\text{-}NMe_2)_2]$ is consistent with the presence of a partial positive charge on the amine nitrogen atoms. Similar dissociation of the triflate ion of the other complexes would generate 16-electron species, which would not be well-stabilized by $CDCl_3$, the solvent used to prepare the NMR samples. The presence of two sets of py-NMe_2 proton signals is unlikely to be due to dissociation of the py-NMe_2 ligands, since, of all the pyridine ligands used, py-NMe_2 is the strongest Lewis base, and hence would be the least likely to dissociate. Moreover, the py-NMe_2 proton signals observed do not correspond to those of the free ligand.

3.3. Crystal structure of $[Re(CF_3SO_3)(CO)_3(py)_2]$

The rhenium atom of $[Re(CF_3SO_3)(CO)_3(py)_2]$ is coordinated octahedrally by three facial CO ligands, two pyridine rings and one triflate ligand (Fig. 3). The Re–C distances *trans* to the pyridine are slightly longer [average 1.904(9) Å] than the Re–C distance *trans* to the triflate [1.881(7) Å]. The distance between the Re atom and the coordinated oxygen of the triflate ligand is 2.194(4) Å, which is similar to distances reported for other rhenium triflate complexes [33,34]. The distance between the coordinated oxygen atom and S1 [1.463(5) Å] is significantly longer than the other two S–O distances [average 1.416(6) Å].

It is noteworthy that the coordination sphere around rhenium is distorted towards trigonal antiprismatic. The average C–Re–C angle [87.7(3)°] between the carbonyl ligands and the average bond angle between the non-carbonyl ligands (L) [83.4(2)°] are significantly smaller than 90°. In contrast, the average angle between carbonyl and non-carbonyl ligands in *cis* configuration [94.4(3)°] is significantly larger than 90°. A search of the Cambridge Crystallographic Database showed that this type of distortion is also present in other $[Re(X)(CO)_3(py)_2]$ complexes, but had not been noted before. On the basis of 11 reported structures [35–45] the average OC–Re–CO, L–Re–L and L–Re–CO angles are 88.5(2)°, 86.3(2)° and 92.6(2)°, respectively [46]. Probably, the repulsion between the Re-carbonyl π-electron clouds and the Re–L σ-electron clouds is stronger than that amongst the Re-carbonyl π-electron clouds and that amongst the Re–L σ-electron clouds. This bond pair–bond pair repulsion between carbonyl and non-carbonyl ligands is apparently stronger than the steric repulsion between the bulky non-carbonyl ligands.

The crystal structure also supports the explanation proposed above for the upfield shift of the pyridine α-proton resonance when the bromide ligand is substituted by triflate. The protons attached to C21 (H21A) and C35 (H35A) are located close to the pyridine rings defined by N2–C35 and N1–C25, respectively, and lie within the shielding regions of the pyridine rings [43] (perpendicular distance to the ring plane = 2.78 Å for H21A and 2.87 Å for H35A; distance to the cen-

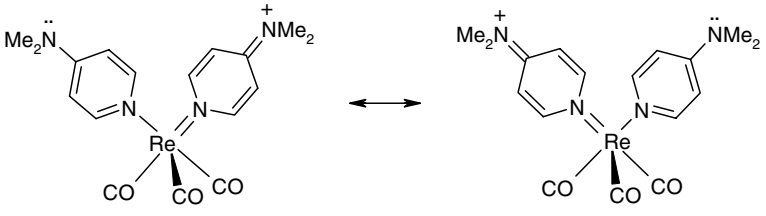

Fig. 2. Two of the resonance structures for the $[Re(CO)_3(py\text{-}NMe_2)_2]^+$ cation.

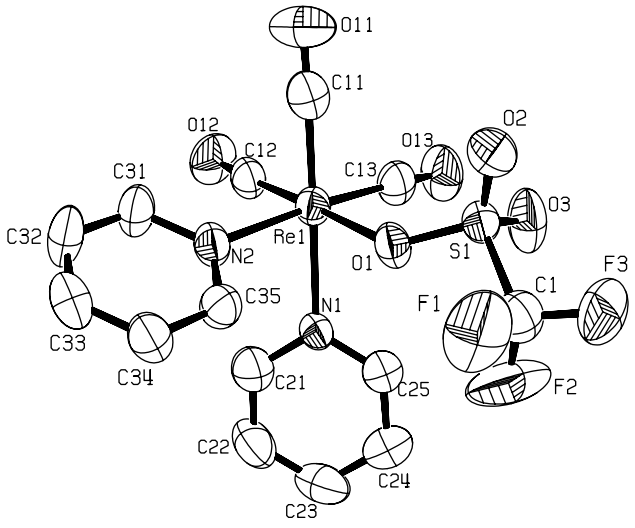

Fig. 3. Molecular structure of $[Re(CF_3SO_3)(CO)_3(py)_2]$ showing the atomic labeling scheme (40% probability ellipsoids). Hydrogen atoms are omitted.

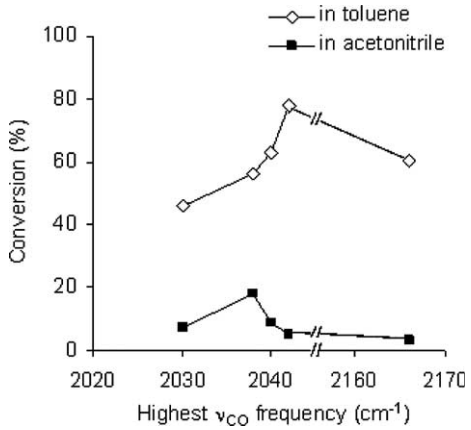

Fig. 4. Conversion of **1** to **3** after 20 h as a function of Lewis acidity of the catalyst precursors $[Re(CF_3SO_3)(CO)_3L_2]$, where L = py-NMe_2, py-Me, py, py-Cl and CO (left to right on the graph). The highest ν_{CO} frequency of the catalyst precursor is used as a measure of its Lewis acidity.

troid = 3.41 Å for H21A and 3.60 Å for H35A, and the projections of H21A and H35A onto the respective ring planes are 1.97 and 2.18 Å from the centroids; the average distance of the centroid from the ring atoms is 1.35 Å). It must be noted, however, that the pyridine rings rotate rapidly in solution, such that both α protons of each ring experience the same shielding by the adjacent ring, hence all the α protons are equivalent on the NMR timescale.

3.4. Catalytic studies

The cyclization reaction of 6-aminohex-1-yne (**1**) to 2-methyl-1,2-dehydropiperidine (**3**) involving the intramolecular addition of an amine group to an alkyne moiety was chosen to test the catalytic activities of the rhenium triflate complexes. The percent conversions of **1** to **3** after 20 h are plotted against the Lewis acidities of the catalyst precursors in Fig. 4.

It is particularly noteworthy that the complexes $[Re(CF_3SO_3)(CO)_3(py\text{-}Me)_2]$ and $[Re(CF_3SO_3)(CO)_3(py\text{-}Cl)_2]$ having intermediate Lewis acidities exhibit the highest catalytic activity when the cyclization reaction is carried out in CH_3CN and toluene, respectively. Such a trend can be described as a 'volcano curve' [47] and it suggests that there is an optimum Lewis acidic strength needed for rhenium-based catalysts to catalyze the hydroamination reaction. If the Re complex is a very weak Lewis acid, the catalyst-substrate complex might be too unstable. On the other hand, if the complex is very acidic, the catalyst-substrate complex is too stable to undergo further reaction. Therefore, a metal centre with an intermediate Lewis acidic strength is preferred.

The conversion obtained for $[Re(CF_3SO_3)(CO)_5]$ (61%) is nearly twice as much as that reported for $[Re(CO)_5(H_2O)]BF_4$ (37%) [16]. This is consistent with the finding that the anion on the transition-metal catalyst has a strong influence on the catalytic activity of the metal complex [16]. Highest activities are observed for complexes containing sulfonate derivatives because these anions have large volumes and relatively low σ-donor strengths. Hence, these anions are weakly coordinated and their metal complexes can dissociate more readily in solution, thus availing the empty coordination site. The triflate anion was also reported to be a suitable anion because of its chemical inertness and the solubility of its complexes in organic solvents.

The rate of conversion of **1** achieved with the chloropyridine complex is comparable to those achieved with other catalysts, e.g., $[Ti(C_5H_5)_2Me_2]$ (**1**/Ti^{4+} molar ratio = 20, toluene, 110 °C, 6 h, 55% yield) [48], $[Cu_2(C_6H_6)(CF_3SO_3)_2]$ (**1**/Cu^+ molar ratio = 100, toluene, 111 °C, 4 h, 100% yield) [19], silica supported *trans*-$[PdMe(NO_3)(PMe_3)_2]$ (**1**/Pd^{2+} molar ratio = 187, CH_3CN, 90 °C, 20 h, 74% conversion) [49], and Zn^{2+} ion-exchanged zeolite Beta (**1**/Zn^{2+} molar ratio = 100, toluene, 111 °C, 8 h, 100% yield) [50].

Much lower conversions (3–18%) were obtained in CH_3CN than in toluene (46–78%), however, which is contrary to the results obtained from other studies, wherein little catalytic inhibition was observed when a coordinating solvent is used [16]. A possible reason for this difference is that, whereas the transition metal complexes used in other studies [16,17] are square planar (coordinatively unsaturated), the rhenium(I) complexes employed in this study are coordinatively saturated. An associative ligand-exchange mechanism is possible for the unsaturated square planar complexes, but not for the saturated Re(I) complexes [51]. For the Re(I)

complexes, substrate binding can only occur on the five-coordinate intermediate $[Re(CO)_3L_2]^+$ generated by the loss of the labile triflate ligand. This intermediate is expected to be present in appreciable concentration in toluene, leading to rapid catalysis. In acetonitrile, however, the vacant site left by the triflate anion would be immediately filled by the solvent molecule, hence catalysis is inhibited.

It is also noteworthy that in CH_3CN, the catalyst precursor with the highest activity is $[Re(CF_3SO_3)(CO)_3(py\text{-}Me)_2]$, whilst in toluene, the stronger Lewis acid $[Re(CF_3SO_3)(CO)_3(py\text{-}Cl)_2]$ has the best catalytic performance. It is believed that the true relationship between intrinsic catalytic activity and Lewis acidity is observed in toluene, whilst in CH_3CN, the substrate-binding site is occupied by CH_3CN, and hence less available for substrate binding. The weaker Lewis acid $[Re(CF_3SO_3)(CO)_3(py\text{-}Me)_2]$ provides the optimum com- promise between ease of solvent dissociation and sufficiently strong substrate binding.

It should also be pointed out that although relative Lewis acidity is clearly an important factor governing the rate of catalysis by $[Re(CF_3SO_3)(CO)_3L_2]$, and that the simplest mechanistic hypothesis consistent with the above observations is, as mentioned earlier, that of alkyne π-coordination followed by amine nucleophilic attack, a pathway involving oxidative addition of the N–H bond cannot be ruled out based on the available data. Oxidative addition of the N–H bond is, however, apparently unprecedented for Re(I) carbonyl complexes. Furthermore, although there have been reports of oxidative addition to Re(I) centres (e.g. [52–54]), as far as we are aware they all involve UV photolysis of η^5-C_5R_5 (R = H, Me) complexes, and are thus of low relevance to the present study.

4. Conclusion

Lewis acidic complexes of rhenium can effectively catalyze the cyclization of 6-aminohex-1-yne to 2-methyl-1,2-dehydropiperidine. To achieve optimum catalytic activity an intermediate Lewis acidity of the rhenium complex is required. Consistent with this conclusion a volcano type curve was observed for the catalytic activity of a series of pyridine-substituted triflato tricarbonyl rhenium(I) complexes of the type *fac*-$[Re(CF_3SO_3)(CO)_3L_2]$ (L = py-Cl, py, py-Me and py-NMe_2). The highest catalytic activity was observed for the complexes *fac*-$[Re(CF_3SO_3)(CO)_3(py\text{-}Me)_2]$ and *fac*-$[Re(CF_3SO_3)(CO)_3(py\text{-}Cl)_2]$ in CH_3CN and toluene, respectively. In general, rhenium complexes are advantageous as catalysts because they are less air and moisture sensitive compared to the f-element and early transition-metal catalysts.

5. Supplementary material

Crystallographic data for the structural analysis has been deposited with the Cambridge Crystallographic Data Centre, CCDC No. 266343 for $[Re(CF_3SO_3)(CO)_3(py)_2]$. Copies of this information may be obtained free of charge from The Director, CCDC, 12 Union Road, Cambridge CB2 1EZ, UK, (fax (int code) +44 1223 336 033 or e-mail: deposit@ccdc.cam.ac.uk or www: http://www.ccdc.cam.ac.uk/).

Acknowledgements

Dr. Eberhardt Herdtweck, Technische Universität München is thanked for searching the Cambridge Crystallographic Database. Funding for this project was provided by the National Institute of Education, Nanyang Technological University.

References

[1] J.J. Brunet, D. Neibecker, in: A. Togni, H. Grützmacher (Eds.), Catalytic Heterofunctionalization: from Hydroamination to Hydrozirconation, Wiley–VCH, Weinheim, 2001, pp. 91–141.
[2] T.E. Müller, M. Beller, Chem. Rev. 98 (1998) 675.
[3] F. Pohlki, S. Doye, Chem. Soc. Rev. 32 (2003) 104.
[4] F. Alonso, I.P. Beletskaya, M. Yus, Chem. Rev. 104 (2004) 3079.
[5] P.W. Roesky, T.E. Müller, Angew. Chem. 115 (2003) 2812.
[6] D. Steinborn, R. Taube, Z. Chem. 26 (1986) 349.
[7] S.W. Benson, Thermodynamical Kinetics: Methods for the Estimation of Thermochemical Data and Rate Parameters, second ed., Wiley, New York, 1976.
[8] J.B. Pedley, R.D. Naylor, S.P. Kirby, Thermochemical Data of Organic Compounds, second ed., Chapman & Hall, London, 1986. Appendix Table 1.2.
[9] V. Khedkar, A. Tillack, M. Beller, Org. Lett. 5 (2003) 4767.
[10] I. Bytschkov, S. Doye, Eur. J. Org. Chem. 6 (2003) 935.
[11] S. Hong, T.J. Marks, Acc. Chem. Res. 37 (2004) 673.
[12] H.M. Senn, P.E. Blöchl, A. Togni, J. Am. Chem. Soc. 122 (2000) 4098.
[13] J. Pawlas, Y. Nakao, M. Kawatsura, J.F. Hartwig, J. Am. Chem. Soc. 124 (2002) 3669.
[14] S. Burling, L.D. Field, B.A. Messerle, P. Turner, Organometallics 23 (2004) 1714.
[15] M. Kawatsura, J.F. Hartwig, J. Am. Chem. Soc. 122 (2000) 9546.
[16] T.E. Müller, M. Grosche, E. Herdtweck, A. Pleier, E. Walter, Y.K. Yan, Organometallics 19 (2000) 170.
[17] T.E. Müller, A. Pleier, J. Chem. Soc., Dalton Trans. (1999) 583.
[18] R.Q. Su, V.N. Nguyen, T.E. Müller, Top. Catal. 22 (2003) 23.
[19] J. Penzien, C. Haeßner, A. Jentys, K. Köhler, T.E. Müller, J.A. Lercher, J. Catal. 221 (2004) 302.
[20] J. Penzien, A. Abraham, J.A. van Bokhoven, A. Jentys, T.E. Müller, C. Sievers, J.A. Lercher, J. Phys. Chem. B 108 (2004) 4116.
[21] T.E. Müller, M. Berger, M. Grosche, E. Herdtweck, F.P. Schmidtchen, Organometallics 20 (2001) 4384.
[22] M. Beller, H. Trauthwein, M. Eichberger, C. Breindl, T.E. Müller, A. Zapf, J. Organomet. Chem. 566 (1998) 277.
[23] M. Beller, H. Trauthwein, M. Eichberger, C. Breindl, T.E. Müller, Eur. J. Inorg. Chem. (1999) 1121.

[24] A. Motta, G. Lanza, I.L. Fragala, T. Marks, J. Organometallics 23 (2004) 4097.
[25] D.F. Shriver, M.A. Dredzon, The Manipulation of Air-sensitive Compounds, second ed., Wiley–Interscience, New York, 1986, p. 7.
[26] J.P. McNally, V.S. Leong, N.J. Cooper, in: A.L. WayDa, M.Y. Darensbourg (Eds.), Experimental Organometallic Chemistry – A Practicum in Synthesis and Characterization, ACS Symposium Series 357, ACS, Washington, DC, 1987, p. 6.
[27] T.E. Müller, J.A. Lercher, V.N. Nguyen, AIChE J. 49 (2003) 214.
[28] S.P. Schmidt, W.C. Trogler, F. Basolo, Inorg. Synth. 28 (1990) 160.
[29] G.M. Sheldrick, SHELXTL PC, Version 5.03, Siemens Analytical X-ray Instruments Inc., Madison, WI, 1994.
[30] D.A. Edwards, J. Marshalsea, J. Organomet. Chem. 131 (1977) 73.
[31] S.P. Schmidt, J. Nitschke, W.C. Trogler, Inorg. Synth. 26 (1989) 113.
[32] K. Nakamoto, Infrared and Raman Spectra of Inorganic and Coordination Compounds, Wiley, New York, 1997.
[33] Re–O 2.206(3) Å for [$Re(CF_3SO_3)(CO)_3\{Ph_2PO(CH_2)_2OPPh_2\}$] M.C. Rodríguez, J. Bravo, E. Freijanes, E. Oñate, S. García-Fontán, P. Rodríguez-Seoane, Polyhedron 23 (2004) 1045.
[34] Re–O 2.186(3) Å for [$Re(CF_3SO_3)(CO)_3$\{2-(2-pyridyl)benzothiazole\}] X. Chen, F.J. Femia, J.W. Babich, J. Zubieta, Inorg. Chim. Acta 314 (2001) 91.
[35] Bromo-tricarbonyl-*trans*-bis(4-(4-(4-dimethylaminophenyl)buta-1,3-dienyl)pyridine)-rhenium dichloromethane solvate, CCD Code FEQJIUO. Briehl, K. Sünkel, I. Krossing, H. Nöth, E. Schmälzlin, K. Meerholz, C. Bräuchle, W. Beck, Eur. J. Inorg. Chem. (1999) 483.
[36] Tricarbonyl-chloro-(1,11-bis(4-yridylcarboxy)-3,6,9-trioxaundecane)-rhenium(I) dichloromethane solvate, CCD Code HOTFEB: S. Belanger, M. Gilbertson, D.I. Yoon, C.L. Stern, X. Dang, J.T. Hupp, J. Chem. Soc., Dalton Trans. (1999) 3407.
[37] Tricarbonyl-chloro-(1,11-bis(4-pyridylcarboxy)-3,6,9-trioxaundecane)-rhenium(I) monohydrate, CCD Code HOTFIF S. Belanger, M. Gilbertson, D.I. Yoon, C.L. Stern, X. Dang, J.T. Hupp, J. Chem. Soc., Dalton Trans. (1999) 3407.
[38] Tetrakis(μ_2-4,4′-bipyridine)-dodecacarbonyl-tetrachloro-tetra-rhenium acetone solvate, CCD Code JOQBAS: S. Belanger, J.T. Hupp, C.L. Stern, R.V. Slone, D.F. Watson, T.G. Carrell, J. Am. Chem. Soc. 121 (1999) 557.
[39] *fac*-Chloro-bis(isoquinoline)-tricarbonyl-rhenium, CCD Code LIFFOV N.M. Iha, G. Ferraudi, J. Chem. Soc., Dalton Trans. (1994) 2565.
[40] Tetrakis(μ_2-4,4′-bipyridine)-bis((1,1′-bis(diphenylphosphino)ferrocene)-platinum(II))-bis(*fac*-bromo-tricarbonyl-rhenium(I))-tetrakis(trifluoromethanesulfonate) nitromethane clathrate, CCD Code MIBSEV S.-S. Sun, J.A. Anspach, A.J. Lees, P.Y. Zavalij, Organometallics 21 (2002) 685.
[41] *fac*-Tricarbonyl-chloro-bis(pyridine-N)-rhenium, CCD Code PUVHIX S. Belanger, J.T. Hupp, C.L. Stern, Acta Crystallogr., Sect. C 54 (1998) 1596.
[42] *fac*-Tricarbonyl-chloro-bis(4,4′-bipyridine-N)-rhenium, CCD Code PUVHOD S. Belanger, J.T. Hupp, C.L. Stern, Acta Crystallogr., Sect. C 54 (1998) 1596.
[43] Tetrakis(μ_2-4,4′-Bipyridine-4,4′-diyl)-dodecacarbonyl-tetrachloro-tetrarhenium acetone solvate, CCD Code TEZHIP: R.V. Slone, J.T. Hupp, C.L. Stern, T.E. Albrecht-Schmitt, Inorg. Chem. 35 (1996) 4096.
[44] *fac*-Bromo-tricarbonyl-bis(4-(ferrocenylethynyl)pyridine)-rhenium dichloromethane solvate, CCD Code TITFOR: J.T. Lin, S.-S. Sun Lin, J.J. Wu, Y.-C. Liaw, K.-J. Lin, J. Organomet. Chem. 517 (1996) 217.
[45] Tricarbonyl-bis(pyridine)-phenylacetylenyl-rhenium, CCD Code VIWAM A.S. Batsanov, Yu.T. Struchkov, V.I. Zhdanovich, P.V. Petrovskii, N.E. Kolobova, Metalloorg. Khim. 2 (1989) 1045.
[46] Cambridge Crystallographic Database, Version 5.25 (November 2003), structural search performed with ConQuest, Version 1.6, Update 2 (April 2004), Update 3 (July 2004); only rhenium complexes with α-H substituted pyridine rings were considered to avoid constraints resulting from steric interactions ([$Re(CF_3SO_3)(CO)_3(py)_2$], FEQJIU, HOTFEB, HOTFIF, LIFFOV, MIBSEV, PUVHIX, PUVHOD, TITFOR with two independent molecules, VIJWAM); the structures JOQBAS and TEZHIP were excluded because of structural disorder.
[47] I. Chorkendorff, J.W. Niemantsverdriet, Concepts of Modern Catalysis and Kinetics, Wiley–VCH, Weinheim, 2003, p. 261.
[48] I. Bytschkov, S. Doye, Tetrahedron Lett. 43 (2002) 3715.
[49] M.K. Richmond, S.L. Scott, H. Alper, J. Am. Chem. Soc. 123 (2001) 10521.
[50] J. Penzien, T.E. Müller, J.A. Lercher, Chem. Commun. (2000) 1753.
[51] M.D. Fryzuk, C.D. Montgomery, Coord. Chem. Rev. 95 (1989) 1.
[52] T.T. Wenzel, R.G. Bergman, J. Am. Chem. Soc. 108 (1986) 4856.
[53] A.H. Klahn, M.H. Moore, R.N. Perutz, J. Chem. Soc., Chem. Commun. (1992) 1699.
[54] F. Godoy, C.L. Higgitt, A.H. Klahn, B. Oelckers, S. Parsons, R.N. Perutz, J. Chem. Soc., Dalton Trans. (1999) 2039.